

Comparative electrochemical study of sulphonated polysulphone binded graphene oxide supercapacitor in two electrolytes

Harish Mudila^{1,2}, M.G.H. Zaidi^{1,*}, Sweta Rana¹ and S. Alam³

¹Department of Chemistry, G. B. Pant University of Agriculture & Technology, Pantnagar 263145, India

²Department of Chemistry, Lovely Professional University, Phagwara 144402, India

³Polymer Division, Defense Materials & Stores Research & Development Establishment (DMSRDE), Kanpur 208013, India

Article Info

Received 29 September 2015

Accepted 22 March 2016

*Corresponding Author

E-mail: mghzaidi@gmail.com

Tel: +919411159853

Open Access

DOI: <http://dx.doi.org/10.5714/CL.2016.18.043>

This is an Open Access article distributed under the terms of the Creative Commons Attribution Non-Commercial License (<http://creativecommons.org/licenses/by-nc/3.0/>) which permits unrestricted non-commercial use, distribution, and reproduction in any medium, provided the original work is properly cited.

Abstract

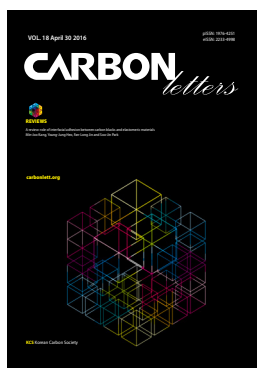
Sulphonated polysulphone (SPS) has been synthesized and subsequently applied as binder for graphene oxide (GO)-based electrodes for development of electrochemical supercapacitors. Electrochemical performance of the electrode was investigated using cyclic voltammetry in 1M Na₂SO₄ and 1M KOH solution. The fabricated supercapacitors gave a specific capacitance of 161.6 and 216.8 F/g with 215.4 W/kg and 450 W/kg of power density, in 1M Na₂SO₄ and 1M KOH solutions, respectively. This suggests that KOH is a better electrolyte than Na₂SO₄ for studying the electrochemical behavior of electroactive material, and also suggests SPS is a good binder for fabrication of a GO based electrode.

Key words: supercapacitor, specific capacitance, sulphonated polysulphone, binder, cyclic voltammetry

1. Introduction

Population growth, industrialization, and continuous decline of traditional fuel reserves have induced serious concern over natural energy production and, for the last few decades, has drawn attention towards prudent ways of storing energy. The present and future demand for production of energy, and efficient systems for its storage, are greater than ever [1,2]. It is also being demanded that that these novel energy sources should involve environmental protection and the judicious replacement of fossil fuels. The energy stored by electronic gadgets requires smooth release with high current delivery whenever conditioned, which is possible only with a high power density device. Supercapacitors, also known as ultracapacitors or electrochemical capacitors, seem to be the best possible contender to meet this requirement because they possess power densities much higher than conventional batteries and much higher energy densities than conventional capacitors [3].

Carbonaceous nanomaterials are among the most promising candidates for applications as supercapacitors owing to their abundance, chemical stability, low cost, fine conductivity, relative environmental friendliness, and the number and variety of allotropic and other forms [1,4]. Among, such carbon based nanomaterials is graphene, a one-atom thick, 2D material composed of sp² hybridized carbon. It is a good candidate for energy storage materials due to its superior electrical conductivity, mechanical properties, thermal conductivity, high surface area, and minimal cytotoxicity. Graphene nanosheets were first obtained by mechanical exfoliation of bulk graphite [5,6]. Further developments have led to graphene, and more generally to graphene oxide (GO). These are synthesized by several chemical methods, like chemical vapor deposition, micro mechanical exfoliation, epitaxial growth, the creation of colloidal suspensions, and inorganic reactions. Chemical means of creating graphene/GO are more viable as these methods are more effective for large-scale manufacturing, leading to the development of devices on a commercial scale [5-7]. GO, existing as individual layered sheets, can be an ideal electrode material as the graphene



<http://carbonlett.org>

pISSN: 1976-4251

eISSN: 2233-4998

Copyright © Korean Carbon Society

sides could be exposed to electrolyte with a potentially large surface area and thus result in high specific capacitance (Cs). It has been also observed that few-layered GO has high electrical conductivity [8,9]. This high conductivity can also be obtained by an electrochemical method. Chemically modified graphene exhibits numerous active edges and functional groups based on oxygen. It has good electrochemical and mechanical properties and that makes them suitable for energy storage devices [7,10].

The preparation and development of stable electrodes needs a binder, which should possess low electrochemical activity, have high electrode stability in the potential range against the reference electrode, exhibit strong adhesion to the current collectors, should prevent possible dendrite formation during cycling, and should also be environmental friendly and non-flammable. In this paper, we describe a new polymeric binder sulphonated polysulphone (SPS) for use in conjunction with GO cathodes. Membranes of SPS have been used successfully in fuel cells due to their very low ion exchange capacity (0.5–1.2 mmol SO₃H/g) and proton conductivities (10⁻⁶ and 10⁻² S cm⁻¹) [11,12]. This low ion exchange capacity has motivated the authors to use SPS membranes in electrochemical electrodes.

The composite cathode materials were fabricated by deposition of a mixture (w/w) comprising binder (25%) combined with GO (65%), and graphite (10%) over 316 SS. These were subjected to cyclic voltammetry (CV) tests in 1M KOH and 1M Na₂SO₄ electrolyte. Capacities of 216.79 and 161.62 F/g, and power density of 450 and 215.4 W/Kg, respectively, was obtained for the two electrolytes. The formation of such synthesized materials has been ascertained using their Fourier-transform infrared spectroscopy (FT-IR) spectra, microscopy, and X-ray diffraction (XRD). This work was performed to identify the impact of the electrolyte on the electrochemical behavior of GO. The results show that 1M KOH is a much better electrolyte for GO-based electrodes.

2. Experimental

2.1. Starting materials

Polysulphone (PSO; M_n 26,000, ρ=1.24 g/cc) and chlorosulfonic acid (bp., 152°C ± 1°C/755 mmHg, ρ = 1.753 g/cc at 25°C) were purchased from Aldrich Chemical Company (St. Louis, MO, USA) and graphite (98.0%, surface area 500 μm) was purchased from Otto Chemicka-Biochemica Reagents (Mumbai, India). All other chemicals and solvents used were obtained from SD Fine Chemicals (Mumbai, India).

2.2. Synthesis of SPS

PSO resin (7.2 g) was poured into a thermostatically controlled, two neck flask maintained at 20°C ± 1°C, equipped with mechanical stirrer and a dripping funnel. Then dichloromethane (DCM; 75 mL) was added to it, the contents were stirred at 100 r/min until the PSO dissolved into the DCM. The funnel was charged with a solution of chlorosulfonic acid in DCM (0.110 g/dL). A solution of chlorosulfonic acid was dripped into the solution of PSO in DCM with constant stirring over 2 h, until

SPS was precipitated. SPS was then filtered out and repeatedly washed with aqueous solution of sodium hydroxide (10%, w/v) for the removal of unreacted chlorosulfonic acid. The SPS was finally washed with de-ionized water and dried at 80°C ± 1°C overnight [13].

2.3. Preparation of GO

GO was prepared according to literature reports via the modified Hummers method. In a typical synthesis, graphite (5 mg, 60 mesh) was subjected to sulfuric acid (120 mL, ρ = 1.84 g/cc at 25°C ± 1°C) at -10°C over 10 min. To this was slowly added potassium permanganate (15 g) under continuous stirring, and maintaining the temperature at 5°C ± 1°C. After 30 min, the ice-bath was removed and the temperature of the contents was allowed to increase to 35°C ± 1°C. De-ionized water (200 mL) was then slowly added to the contents, causing an increase in temperature to 98°C ± 1°C. After that, hydrogen peroxide (30%, 50 mL) was added to the contents to reduce the residual KMnO₄. The contents were further diluted with warm de-ionized water (450 mL) and treated with hydrochloric acid (5%, 50 mL). The mixture was then filtered and the residue was washed with de-ionized water, until the filtrate became neutral and free from salt impurities. The GO was dried at 45°C ± 1°C and 400 mmHg (53.329 kPa) over 48 h.

2.4. Fabrication of electrodes

The working electrodes were fabricated by mixing the electroactive material along with graphite and SPS binder in N-Methylpyrrolidone (NMP) in the percentage ratio (65:10:25), over a 1 cm² SS substrate. Prior to the application of content (50 μL) over SS, they were ultrasonicated for 15 min. The treated substrate was dried at room temperature for 4–5 h, followed by 100°C at 400 mmHg for 48 h. The result was creation of cathodes with mass thickness of 0.5 mg electroactive materials over the SS substrate.

2.5. Characterization

Scanning electron microscope (SEM) images of the gold coated GO were recorded using a JEOL (JSM-6610 LV, JEOL, Japan) with beam voltage 5 kV at 2.7 KX, 5 μm. XRD patterns of the powdered samples were recorded at room temperature using a Rigaku-Geigerflex X-Ray Diffractometer (Japan) with Cu-Kα radiation. FT-IR spectra were recorded on a Thermo Nicolet FT-IR Spectrophotometer (USA) using KBr pellets. All electrochemical measurements were scanned using an IVIUM potentiostat-galvanostat (Netherlands BV) at current compliance 10 mA, and ranges of voltage compliance -0.2 to 0.2 V and -0.3 to 0.2 V for 1.0M Na₂SO₄ and 1.0M KOH respectively, at scan rate of 0.001 to 0.15 V/s using a three-electrode cell assembly with reference to a Ag/AgCl electrode. Pt foil with 1 cm² area was used as counter electrode and a commercially available 316-SS electrode as a working electrode. Specific capacitance (Cs) of the active material was calculated from the voltammetric charges by the CV curve, by means of the relation:

$$C_s(F/g) = \frac{q_a + |q_c|}{2m\Delta V} \quad (1)$$

where q_a and q_c are the voltammetric charges on the anodic and cathodic scans, in the capacitive potential region (ΔV), and with m being the mass of active material.

3. Results and Discussion

3.1. FT-IR spectra

The various functional groups that enhance the pseudocapacitance behavior of the oxidized material were analyzed employing the FT-IR spectra shown in Fig. 1. GO consists of covalently attached oxygen-containing groups such as hydroxyl, epoxy, carbonyl, and carboxyl groups. Considering the structure of GO, it is generally accepted that the epoxy and C-OH functional groups are attached above and below each carbon layer (the basal plane), while the COOH groups are bound to the edges of the basal planes. It has been reported [10] that the functional groups and heteroatoms on the carbon sheets improve the wettability of electrodes due to an increased number of hydrophilic polar sites and thus enhances the overall capacitance of the electrodes.

The formation of GO was verified using FT-IR spectra. Fig. 1 shows FT-IR spectra of graphite (Fig. 1a) and GO (Fig. 1b). Graphite revealed characteristic absorptions at 3447.28 (ν O-H)

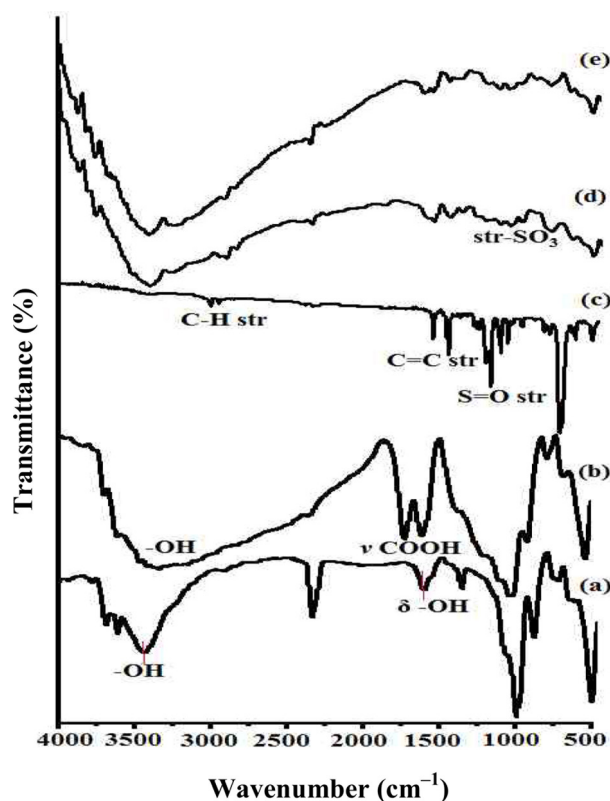


Fig. 1. Fourier-transform infrared spectroscopy spectra of graphite (a), graphene oxide (GO) (b), polysulphone (c), sulphonated polysulphone (SPS) (d), and SPS/GO (e).

and 1628.79 (δ O-H), which were attributed to the presence of absorbed moisture [14]. GO indicated characteristic absorptions at \sim 3333 (ν O-H), 1723 (ν COOH), 1613 (remaining sp^2 -character), 1378 (ν COC), 1221.20 (C-O for oxirane), and 1033 (ν COH) [15,16]. Fig. 1c shows characteristic peaks at 1295 (S=O str), 1411–1580 (C=C str) and 2870–2950 cm^{-1} (C-H str) for PSO. The sulfonation process of the polysulphone polymer was confirmed qualitatively by FT-IR. The results indicated clearly the presence of sulfonic groups in the polymer backbone after the sulfonation reaction occurred. This can be observed at 1020 cm^{-1} in Fig. 1d, and is the evidence of the SO_3 stretching of the sulfonic groups. However, the presence of a sulfonic acid group peak can be seen clearly in the predicted region. The SO_2 symmetric stretching was clearly observed at 1160 cm^{-1} and a para in-plane aromatic C-H bend could be detected at 1100 cm^{-1} [17]. In contrast, different trends of the spectra were observed when the SPS was hydrated. A water absorption effect of the membrane samples could be seen clearly in Fig. 1d where the O-H stretching band of the SPS sample was detected at frequency \sim 3220 to 3560 cm^{-1} . SPS created a broad stretching band, indicating greater amounts of water. This effect was presumed to be associated with increasing hydrophilic behavior due to the introduction of the sulfonate group in the polymer structure. The results of FT-IR analysis clearly demonstrated the occurrence of sulfonation by the presence of sulfonate groups after the reaction in the polymer backbones [18]. Fig. 1e shows all the major peaks corresponding to GO and SPS, and showing conjunction between the two.

3.2. X-ray diffraction

Typical XRD patterns of as-synthesized GO (Fig. 2b) and graphite (Fig. 2a) are shown in Fig. 2. The graphite shows an intensive peak around $2\theta = 26.427^\circ$ ($d = 3.369 \text{ \AA}$), reduced to $2\theta = 11.829^\circ$ ($d = 7.473 \text{ \AA}$), which indicates greater interlayer spacing in GO, and also exfoliation of the graphite into GO [19,20]. The oxidation process results in the insertion of hydroxyl and epoxy groups between the carbon sheets, mainly at the centers while the carboxyl groups are inserted on the terminal and lateral sides of the sheets. The insertion of these groups leads to decreased van der Waals forces between the graphene sheets in GO.

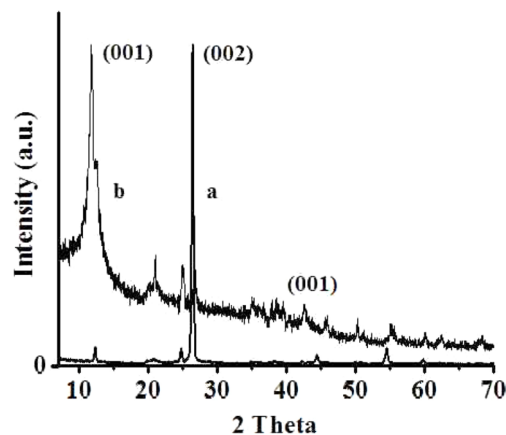


Fig. 2. X-ray diffraction spectra of graphite (a) and graphene oxide (b).

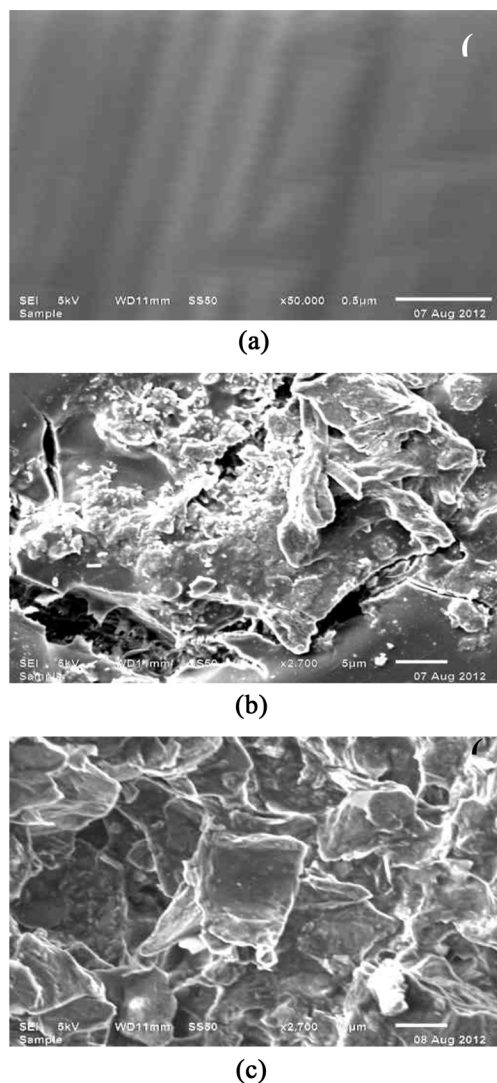


Fig. 3. Scanning electron microscope images of bare SS (a), sulphonated polysulphone (b), and graphene oxide over SS (c).

3.3. Scanning electron microscope

SEM revealed a characteristic polished surface of SS with the emery paper at 50 KX at 0.5 μm (Fig. 3a). The SS surface had a rough texture due to emery paper treatment during preparation of the electrode. The SPS microstructure is presented in Fig. 3b at 2.7 KX at 5 μm . The SPS showed fine distribution of grains, with clogging due to phase separation during the evaporation process of NMP in air. Such clogs in the SPS microstructure might have formed due to the nucleation phenomena of SPS. Blending of GO (% w/w) with SPS produced a composite material in which GO has a flaky appearance, with a rough surface and non-uniform grain distribution (Fig. 3c).

3.4. Electrochemistry

The electrochemical properties of SPS over SS were studied via CV in a three-electrode cell configuration at room tem-

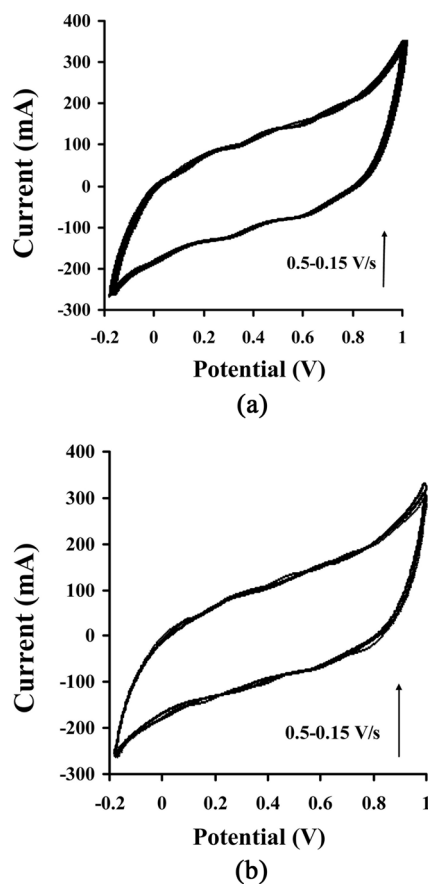


Fig. 4. (a) Cyclic voltammetry (CV) of sulphonated polysulphone vs. Ag/Ag^+ electrode at various scan rates in 1M KOH. (b) CV of sulphonated polysulphone vs. Ag/Ag^+ electrode at various scan rates in 1M Na_2SO_4 .

perature in 1M KOH and 1M Na_2SO_4 at a common scan rate of 0.05, 0.1, and 0.15 V/s, in the potential region of -0.2 to 1.0 V vs. Ag/AgCl . The result suggests that SPS shows poor electrochemical behavior, and exhibited its highest C_s of 0.31 F/g and 0.29 F/g with KOH and Na_2SO_4 electrolytes, respectively (Fig. 4). The electroactive characteristics of GO was clearly observed through redox reactions associated with GO, as shown in CV. Redox transitions between a semiconducting state and a conducting state are responsible for cathodic and anodic peaks. The CV curves of the GO electrode clearly shows faradaic redox reactions, which exhibit anodic peaks associated with the oxidation of GO, and a cathodic peak corresponding to reduction of GO. At this scan rate, all such I/V compliances were found to consist of increasing peak current and a shift in the voltage to higher values. The peak potential shift in CV is probably due to slow ion diffusion or interfacial charge transfer processes. In a CV, the higher the redox peaks, the greater the electrochemical reaction activity [21,22].

The scanning of SPS-bound GO was performed in the voltage ranges of -0.2 to 0.2 V and -0.3 to 0.2 V, in 1M Na_2SO_4 and 1M KOH solutions, respectively, at various scan rates (0.001–0.15 V/s) for the capacitor cell (Fig. 5). The charging and discharging cyclic voltammograms were observed to be close to a rectangular shape and there was no current

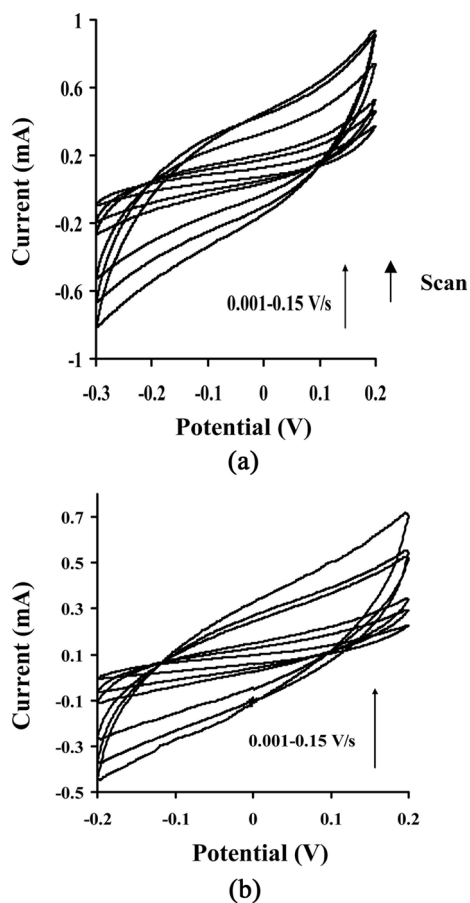


Fig. 5. (a) Effect of scan rate on cyclic voltammetry (CV) of graphene oxide (GO) vs. Ag/Ag⁺ in 1M KOH. (b) Effect of scan rate on CV of GO vs. Ag/Ag⁺ in 1M Na₂SO₄.

peak caused by a redox reaction, indicating typical capacitive behavior with good charge propagation. With this scan rate, a regular increase in the peak currents was observed for GO. The I/V characteristics of GO displayed a range for cathodic and anodic currents (using calculations based on I/V characteristics with scan rate), which revealed that the Cs of GO ranged from 161.62 to 2.96 F/g, and 216.79 to 5.38 F/g, in 1M Na₂SO₄ and 1M KOH solutions, respectively. There was no significant capacitance fading for the initial several cycles. At a high scan rate, diffusion of electrolyte ions was limited due to the time constraint, and only the outer active surface was utilized for charge storage. The maximum Cs of GO was 216.79 F/g at scan rate 0.001 V/s in 1M KOH solution. There was a capacitive decrease of ~2.5% during the first 1000 cycles at a scan rate of 0.1 V/s (Fig. 6a). In 1M Na₂SO₄ solution, GO showed capacitive retention of ~99% (Fig. 6b), indicating the excellent cyclic stability of GO for supercapacitor applications.

The maximum energy density (E) and power density (P) at 0.001 V/s for GO in both electrolytes, were estimated (respectively) using the following equations:

$$E(\text{Wh/Kg}) = \frac{Cs(\Delta V)^2}{2} \quad (2)$$

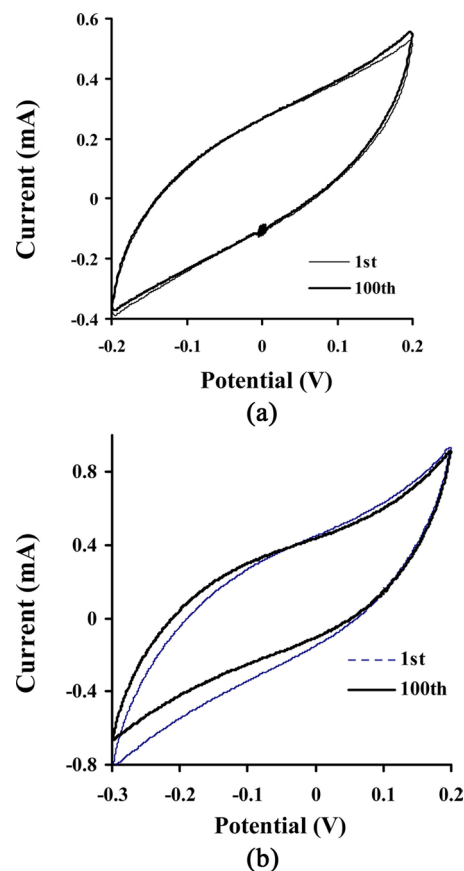


Fig. 6. (a) Cyclic voltammetry (CV) of graphene oxide (GO) vs. Ag/Ag⁺ at 0.1 V/s up to 100 cycles in 1M Na₂SO₄. (b) CV of GO vs. Ag/Ag⁺ electrode at various scan rates in 1M KOH.

$$P(\text{W/Kg}) = \frac{E}{t} \quad (3)$$

where Cs is specific capacitance, ΔV is the applied initial voltage and t is the corresponding discharge time in hours. The maximum energy densities in Na₂SO₄ and KOH were 3.6 Wh/kg and 7.5 Wh/kg, while the corresponding power densities were 215.4 W/kg and 450.0 W/kg.

The Cs in 1M Na₂SO₄ was relatively low, which could be attributed to the nature of the electrolyte. To obtain the maximum power performance for an electrochemical capacitor, the internal electrical resistance in the capacitor must be minimized. This could be achieved by maximizing the conductance of the electrolyte, which provides the basis for double-layer capacitance, or for the Faradaic processes associated with charge or discharge of pseudocapacitance. The ionic conductivity of Na⁺ is lower than that of K⁺; so the ionic conductivity of 1M Na₂SO₄ electrolyte is lower than that of 1M KOH. Another factor could be that the functional groups attached to graphene nanosheets are more chemically active in alkaline electrolytes where redox reactions occurred. In 1M Na₂SO₄ and 1M KOH electrolytes, redox peaks are clearly visible, indicating the participation of functional groups in electrochemical activities and the contribution of pseudocapacitance.

4. Conclusions

GO synthesized via modified Hummers method was employed for a supercapacitance study using two different electrolytes. Studies based on SEM, FT-IR, and XRD spectra revealed the perfect formation of GO. The electrochemical behavior of GO in the two electrolytes (i.e., 1M KOH and 1M Na₂SO₄) was indicated using CV at a common scan rate in the range 0.001–0.15 V/s. The CV scan of GO in 1M KOH shows higher Cs, energy and power densities in comparison to 1M Na₂SO₄ electrolyte at all the rates of scanning. This suggests that KOH is a better electrolytic solution than Na₂SO₄. There was also a ~0.5% capacitive decrease after 1000 successive scans for 1M KOH, providing stability to the electroactive cathode material bound with SPS. The obtained results suggest that SPS shows poor electrochemical behavior, with Cs 0.31 to 0.29 F/g. There was also good adhesion to the current collectors, which prevented possible dendrite formation during cycling. It was also environmentally friendly and non-flammable, being kept for 48 h at 100°C.

Conflict of Interest

No potential conflict of interest relevant to this article was reported.

Acknowledgements

The financial assistance provided by a DRDO vide grant, reference No.ERIP/ER/0703649/M/01/1092, and a DST Inspire fellowship are acknowledged.

References

- [1] Ghosh A, Lee YH. Carbon-based electrochemical capacitors. *ChemSusChem*, **5**, 480 (2012). <http://dx.doi.org/10.1002/cssc.201100645>.
- [2] Choi HJ, Jung SM, Seo JM, Chang DW, Dai L, Baek JB. Graphene for energy conversion and storage in fuel cells and supercapacitors. *Nano Energy*, **1**, 534 (2012). <http://dx.doi.org/10.1016/j.nanoen.2012.05.001>.
- [3] Yoo HM, Heo GY, Park SJ. Effect of crystallinity on the electrochemical properties of carbon black electrodes. *Carbon Lett*, **12**, 252 (2011). <http://dx.doi.org/10.5714/CL.2011.12.4.252>.
- [4] Singh V, Joung D, Zhai L, Das S, Khondaker SI, Seal S. Graphene based materials: past, present and future. *Prog Mater Sci*, **56**, 1178 (2011). <http://dx.doi.org/10.1016/j.pmatsci.2011.03.003>.
- [5] Wu ZS, Zhou G, Yin LC, Ren W, Li F, Cheng HM. Graphene/metal oxide composite electrode materials for energy storage. *Nano Energy*, **1**, 107 (2012). <http://dx.doi.org/10.1016/j.nanoen.2011.11.001>.
- [6] Zhao H, Pan L, Xing S, Luo J, Xu J. Vanadium oxides-reduced graphene oxide composite for lithium-ion batteries and supercapacitors with improved electrochemical performance. *J Power Sources*, **222**, 21 (2013). <http://dx.doi.org/10.1016/j.jpowsour.2012.08.036>.
- [7] Wan C, Chen B. Reinforcement and interphase of polymer/graphene oxide nanocomposites. *J Mater Chem*, **22**, 3637 (2012). <http://dx.doi.org/10.1039/C2JM15062J>.
- [8] Li ZJ, Yang BC, Zhang SR, Zhao CM. Graphene oxide with improved electrical conductivity for supercapacitor electrodes. *Appl Surf Sci*, **258**, 3726 (2012). <http://dx.doi.org/10.1016/j.apsusc.2011.12.015>.
- [9] Gómez-Navarro C, Weitz RT, Bittner AM, Scolari M, Mews A, Burghard M, Kern K. Electronic transport properties of individual chemically reduced graphene oxide sheets. *Nano Lett*, **7**, 3499 (2007). <http://dx.doi.org/10.1021/nl072090c>.
- [10] Karthika P, Rajalakshmi N, Dhathathreyan KS. Functionalized exfoliated graphene oxide as supercapacitor electrodes. *Soft Nanosci Lett*, **2**, 59 (2012). <http://dx.doi.org/10.4236/snsl.2012.24011>.
- [11] Lufrano F, Squadrito G, Patti A, Passalacqua E. Sulfonated polysulfone as promising membranes for polymer electrolyte fuel cells. *J Appl Polym Sci*, **77**, 1250 (2000). [http://dx.doi.org/10.1002/1097-4628\(20000808\)77:6<1250::AID-APP9>3.0.CO;2-R](http://dx.doi.org/10.1002/1097-4628(20000808)77:6<1250::AID-APP9>3.0.CO;2-R).
- [12] Lufrano F, Gatto I, Staiti P, Antonucci V, Passalacqua E. Sulfonated polysulfone ionomer membranes for fuel cells. *Solid State Ionics*, **145**, 47 (2001). [http://dx.doi.org/10.1016/S0167-2738\(01\)00912-2](http://dx.doi.org/10.1016/S0167-2738(01)00912-2).
- [13] Mudila H, Joshi V, Rana S, Zaidi MGH, Alam S. Enhanced electrocapacitive performance and high power density of polypyrrole/graphene oxide nanocomposites prepared at reduced temperature. *Carbon Lett*, **15**, 171 (2014). <http://dx.doi.org/10.5714/CL.2014.15.3.171>.
- [14] Bourdo SE, Viswanathan T. Graphite/polyaniline (gp) composites: synthesis and characterization. *Carbon*, **43**, 2983 (2005). <http://dx.doi.org/10.1016/j.carbon.2005.06.016>.
- [15] Bissessur R, Liu PKY, Scully SF. Intercalation of polypyrrole into graphite oxide. *Synth Met*, **156**, 1023 (2006). <http://dx.doi.org/10.1016/j.synthmet.2006.06.024>.
- [16] Wang K, Ruan J, Song H, Zhang J, Wo Y, Guo S, Cui D. Biocompatibility of graphene oxide. *Nanoscale Res Lett*, **6**, 1 (2011). <http://dx.doi.org/10.1007/s11671-010-9751-6>.
- [17] Wei X, Wang Z, Wang J, Wang S. A novel method of surface modification to polysulfone ultrafiltration membrane by preadsorption of citric acid or sodium bisulfite. *Membr Water Treat*, **3**, 35 (2012). <http://dx.doi.org/10.12989/mwt.2012.3.1.035>.
- [18] Naim R, Ismail AF, Saidi H, Saion E. Development of sulfonated polysulfone membranes as a material for Proton Exchange Membrane (PEM). *Proceedings of Regional Symposium on Membrane Science and Technology, Johor Bharu* (2004). <http://eprints.utm.my/1037/>.
- [19] Xiao P, Xiao M, Liu P, Gong K. Direct synthesis of a polyaniline-intercalated graphite oxide nanocomposite. *Carbon*, **38**, 626 (2000). [http://dx.doi.org/10.1016/S0008-6223\(00\)00005-1](http://dx.doi.org/10.1016/S0008-6223(00)00005-1).
- [20] Chen C, Yang QH, Yang Y, Lv W, Wen Y, Hou PX, Wang M, Cheng HM. Self-assembled free-standing graphite oxide membrane. *Adv Mater*, **21**, 3007 (2009). <http://dx.doi.org/10.1002/adma.200803726>.
- [21] Jeong HK, Jin M, Ra EJ, Sheem KY, Han GH, Arepalli S, Lee YH. Enhanced electric double layer capacitance of graphite oxide intercalated by poly(sodium 4-styrenesulfonate) with high cycle stability. *ACS Nano*, **4**, 1162 (2010). <http://dx.doi.org/10.1021/nn901790f>.
- [22] An KH, Jeon KK, Heo JK, Lim SC, Bae DJ, Lee YH. High-capacitance supercapacitor using a nanocomposite electrode of single-walled carbon nanotube and polypyrrole. *J Electrochem Soc*, **149**, A1058 (2002). <http://dx.doi.org/10.1149/1.1491235>.